

# Color Management for Color Facsimile

*Jon Yngve Hardeberg, Francis Schmitt, Ingeborg Tastl, Hans Brettel and  
Jean-Pierre Crettez*

*Ecole Nationale Supérieure des Télécommunications, Département Images  
Paris, France*

## Abstract

We propose a color management system for the color facsimile. It consists of protocols for the colorimetric calibration of the scanner and the printer by establishing the relationships between the device-dependent color coordinates and the device-independent CIELAB color space. The scanner calibration is based on 3rd order polynomial regression techniques. The printer calibration uses 3D triangulation techniques, which gives us high flexibility and which allows us to apply different color gamut mapping techniques in an efficient way. The online color transformations are calculated by a tetrahedral interpolator using 3D look-up tables provided by the calibration algorithms.

## Introduction

The first international standard for color facsimile was approved in 1994.<sup>1</sup> It fixed JPEG as the encoding method for continuous-tone color images and chose the CIELAB<sup>2</sup> color space with CIE Standard Illuminant D50<sup>3</sup> as the default color space for data transmission.

An important aspect of color facsimile products is the quality of the color reproduction. To obtain faithful color reproduction, colorimetric calibration of the I/O devices is needed, so that the device-dependent color coordinates of the scanner, the printer and the monitor can be linked to the device-independent CIELAB color space. Furthermore, efficient means for processing and converting images are needed. These are typically the tasks performed by a color management system.<sup>4</sup>

To calibrate I/O devices colorimetrically, three different approaches are typically used:

- **Theoretical/physical Models.** Classical examples of this approach are the Neugebauer printer model,<sup>5</sup> and the monitor models based on relatively few parameters such as the specification of the chromaticity coordinates and gamma value of each channel, and the specification of the white point.<sup>6</sup> The drawback with such models is that they are mostly technology dependent.
- **Analytical Models.** They are based on the minimizing of the mean square error of a set of measurement points by polynomial regression. These models are widely used, especially for input devices such as scanners.<sup>7</sup> Important design parameters for this approach are the polynomial order as well as the choice of input/output color spaces requiring pre/post-processing.

- **Geometric Models.** Such models are based on lookup-tables and interpolations. They are used by numerous authors,<sup>8,9,10</sup> and have the advantage to be general. However, they require mostly a larger amount of measured data, compared to the precedent models.

We present a color management system for the color facsimile, consisting of procedures for the colorimetric calibration of the scanner, based on an analytical model, as well as for the calibration of the printer, based on a geometric model. The calibration of the monitor, based on a simple physical model of a CRT display is quite straightforward, and will not be presented in this document.

## Methodology

The proposed methodology is composed of two steps, *i*) a colorimetric calibration of the scanner and the printer done offline from time to time, *ii*) the color transformations done online for the scanned image to be transmitted and for the received image to be printed or displayed on a monitor. The calibration step provides 3D look-up tables which are used to perform the online color conversions.

### Online Color Conversions.

All the color conversions are performed by the use of look-up tables and tetrahedral interpolation, as shown in Figure 1. This strategy presents the main advantage to be general, when compared to device-specific algorithms; only one conversion engine is needed for all types of conversions. It can therefore easily be implemented using either a single software procedure, or a dedicated hardware. Furthermore, an interpolation scheme requires less computational power than most of the conversion algorithms based on physical or analytical models.

In our approach, the central computation engine is a 3D tetrahedral interpolation algorithm which works on a regular cubic mesh.<sup>11</sup> It presents the advantage over a conventional tri-linear interpolator in that it computes a barycentric combination over only 4 vertices (4 multiplications, 3 additions per channel) instead of 8 vertices (8 multiplications, 7 additions per channel) in the tri-linear case. An important design choice is the size of the look-up table containing the final values to be interpolated at the vertices of the regular mesh. In our implementation we have chosen a 33×33×33 cubic mesh. In the next sections, we will discuss the procedures providing the actual values for these look-up tables.

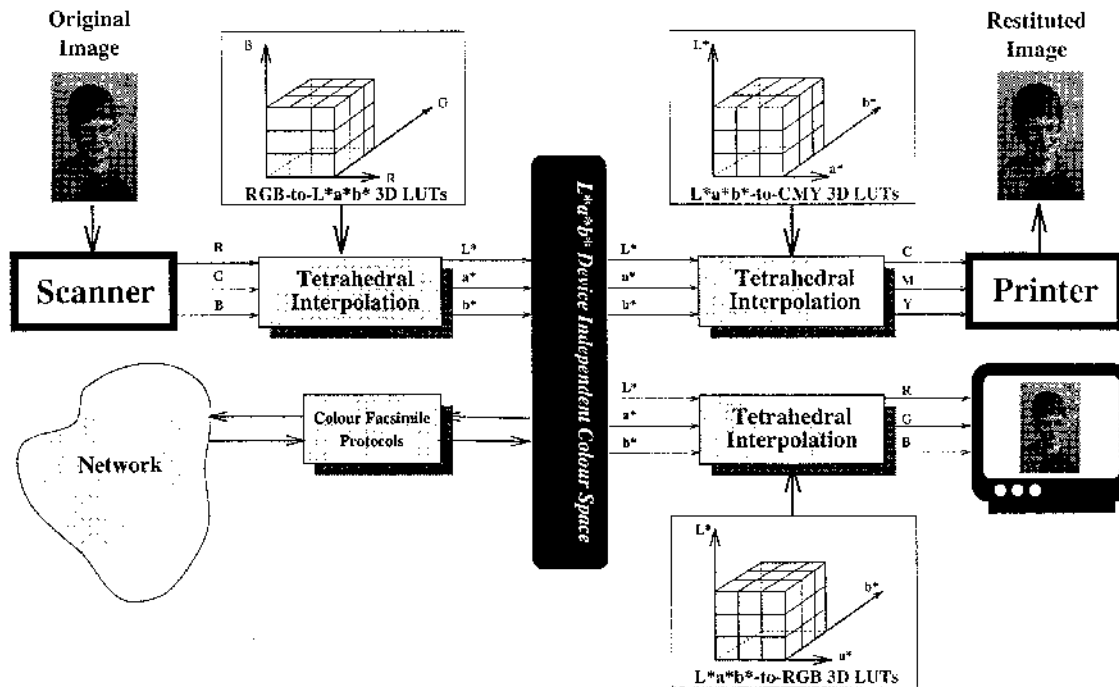


Figure 1. A color facsimile system. The transformations between device dependent color coordinates (RGB and CMY) and the CIELAB color space is performed using 3D look-up tables and a tetrahedral interpolation technique.

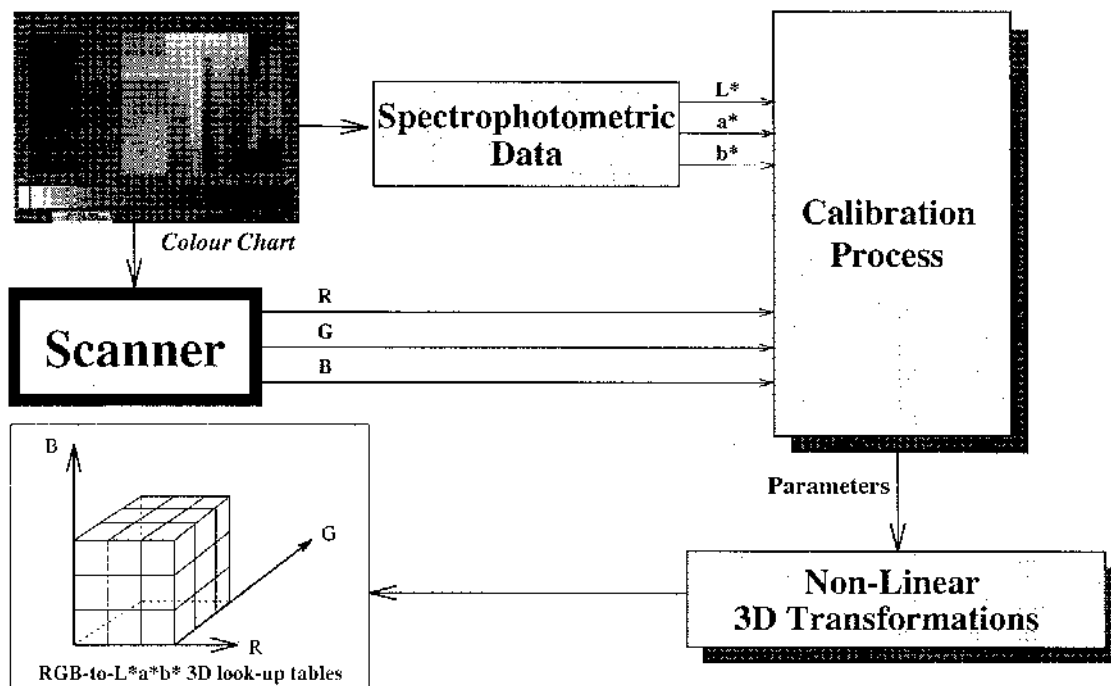


Figure 2. The scanner calibration process, providing a 3D lookup-table for the conversion from scanner RGB to CIELAB.

**Scanner Calibration.**

For the scanner calibration we propose an analytical model, based on a polynomial regression and the minimization of  $\Delta E_{ab}$ .

The calibration is done as follows, see Figure 2. We dispose of an IT8.7/2 color chart,<sup>12</sup> which contains 288 color samples with known CIELAB values. This chart is scanned, and by a picture processing routine we segment each color sample and calculate the mean values of its RGB

scanner components. In order to calibrate the scanner we want to define a 3D nonlinear transformation  $[L^*, a^*, b^*] = f(R, G, B)$ , which converts the RGB components into CIELAB values. Different non-linear transformations with one or several successive internal steps might be chosen. For the main step we use  $n$ th order polynomials whose coefficients may be optimized by a standard regression technique.<sup>13</sup> We can add other steps before and after the main one by using pre-defined non-linear transformations (as gamma-corrections for example). We have tested and compared various schemes.<sup>14,15,16</sup> The retained method consists of using 3rd order polynomials applied on the cubic root of the RGB values. This preprocessing serves as a first approximation of the cubic root function involved in the conversion from CIEXYZ to CIELAB.

This transformation gives satisfactory results; applied on an AGFA Arcus II scanner, we obtained a mean error of  $\Delta E_{ab} = 1.01$ , and a maximum error of  $\Delta E_{ab} = 5.52$  between the computed and the measured CIELAB values on the complete set of patches of the IT8.7/2 chart.

To evaluate the result of our calibration process, it would be interesting to compare the error in terms of  $\Delta E_{ab}$  with and without calibration, that is, for each patch of the color chart, to compare the CIELAB-values obtained by our calibration with the CIELAB-values obtained *without* calibration. This is, however, not a straightforward task, the problem being how to obtain “good” *uncalibrated* CIELAB-values. In the absence of a calibration procedure, a natural approach would be to follow what a typical user probably would do, by first adjusting the gamma corrections at the scanning step in order to choose the preferred image to the screen and then by considering the scanned image as it appears on the screen as a reference. With this in mind, it makes sense to define the *uncalibrated* transformation from gamma corrected RGB scanner to CIELAB as the transformation between the RGB space of a standard monitor and CIELAB.

For the uncalibrated transformation we chose a gamma correction of 2.2 at the scanner step, and then applied our CRT model, this giving a mean error of  $\Delta E_{ab} = 9.18$  and a maximum error of  $\Delta E_{ab} = 26.1$ . Figure 3 shows the error histograms for a calibrated and an uncalibrated system, respectively. We see that the calibration process introduces a significant improvement of the colorimetric quality of the scanner.

### Printer calibration.

The printer calibration is somewhat more complicated than for the scanner, for various reasons. First, we have to consider the color gamut of the printer. Gamut mapping techniques are needed to bring out-of-gamut colors inside

the color gamut. Numerous algorithms have been proposed.<sup>17,18,19</sup> Furthermore, the output space (CMY) of the printer is not a perceptually uniform space. This is in contrast to the scanner calibration process where the output space was CIELAB. Thus a solution based on polynomial regression is not suitable, since the mean square error minimized by the regression is no longer expressed in terms of  $\Delta E_{ab}$ .

We present a geometrical method where the calibration process defines a 3D look-up table for the transformation from CIELAB to CMY taking into account both the colorimetric calibration of the printer, and the color gamut mapping.

Our method, as presented in Figure 4, consists of first sending a numerical color chart to the printer, with patches containing CMY values covering the entire printer color gamut. Then we analyse the printed chart to obtain the CIELAB values corresponding to each patch. This analysis can be done either by a calibrated scanner, or by using a spectrophotometer if available. When this is done, we dispose of the CIELAB values, and the corresponding CMY values, for each color of the chart. From this data set, we construct a 3D Delaunay triangulation<sup>20</sup> in CMY space, which we then export to CIELAB space. By using a Delaunay triangulation we are not limited to using colors lying on a regular grid in the CMY space, as would be the case with regular triangulation techniques.<sup>9</sup> This implies that we can use colors that are more regularly distributed in the CIELAB space, and that we can add more colors in regions where the eye is more sensitive, for example grays or skin tones. A natural choice of color chart would be the IT8.7/3 chart.<sup>21</sup>

At this point we dispose of a segmentation in tetrahedra of the part of the CIELAB space lying inside the printer color gamut, see Figure 5. In order to be able to treat out-of-gamut colors, we have added an englobing structure by projection from a central point, in such a way that we can navigate in the entire CIELAB space, both inside and outside the printer gamut. Now, all possible CIELAB values are contained in this extended 3D structure, and we can use this structure to implement in an elegant, efficient and quick way different gamut mapping techniques, like clipping, gamut compression, white point adaption etc. Both image-dependent and image-independent methods are feasible.

This 3D triangulation approach allows to calculate, by tetrahedral interpolation, the transformation from CIELAB to CMY values for any point of the CIELAB space. We compute this transformation for all the vertices of the regular grid composing the look-up table which will be used for the online color conversion.

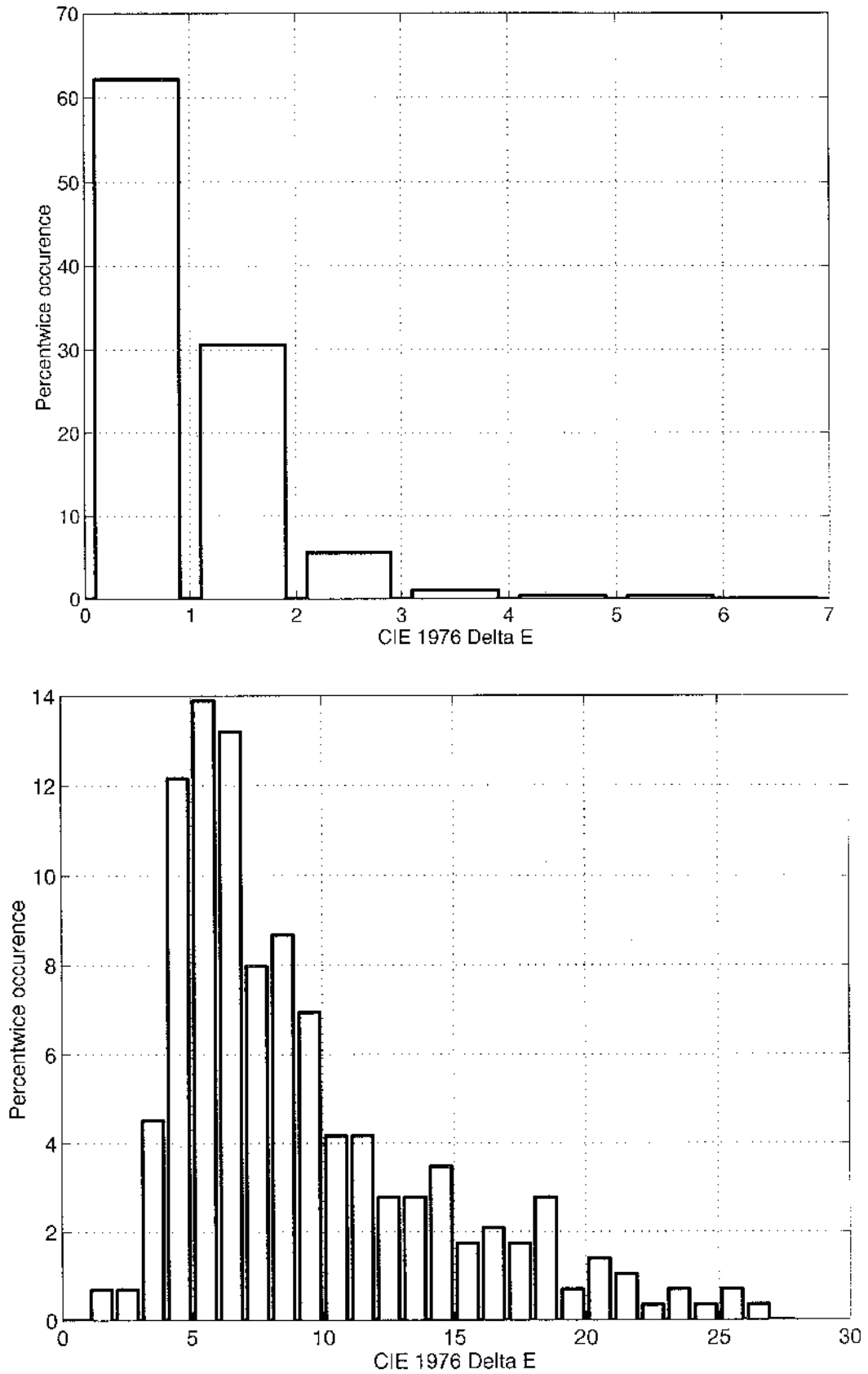


Figure 3. Error histograms for the FUJI IT8.7/2 chart with and without calibration.

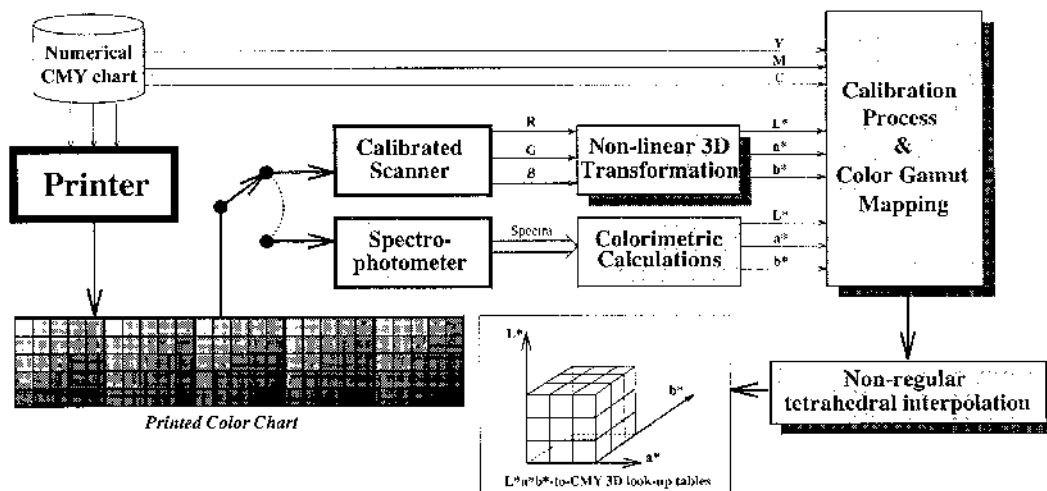


Figure 4. The printer calibration process, providing a 3D lookup-table for the conversion from CIELAB to CMY.

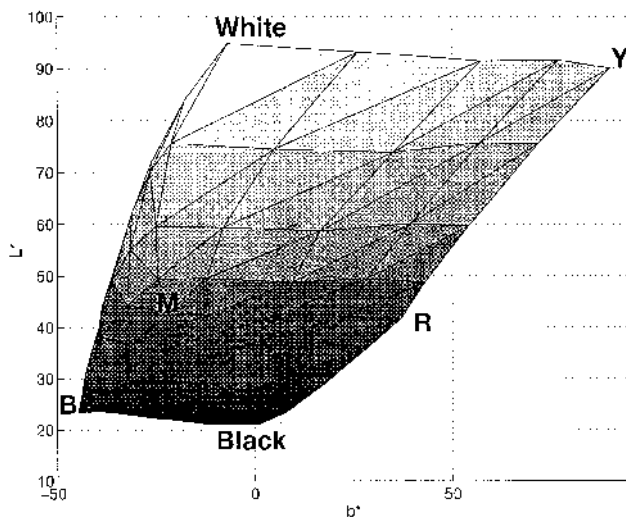


Figure 5. A CIELAB view of the triangulated color gamut of the Mitsubishi S340-10 sublimation printer, built on a regular  $5 \times 5 \times 5$  color chart.

## Conclusion

The proposed color management system for color facsimile presents several interesting features. First its flexibility and homogeneity: each device is characterized by a 3D look-up table and the same simple color transformation process (a tetrahedral interpolator) is used for the scanner, the printer, and the monitor.

The scanner calibration based on polynomial regression provides good results in terms of  $\Delta E_{ab}$ . The printer calibration based on 3D triangulation techniques is particularly well adapted to embed directly various gamut mapping algorithms.

## References

1. ITU-T Rec. T.42. *Continuous-tone colour representation method for facsimile*, November 1994.

2. CIE Publ. No. 15.2. *Colorimetry*, 2nd ed., 1986.
3. G. Wyszecki and W. S. Stiles. *Color Science—Concepts and Methods, Quantitative Data and Formulae*, 2nd ed., John Wiley, New York, 1982.
4. L.W. MacDonald. *Device independent colour reproduction*, Seminar Lecture Notes, SID Eurodisplay '93, pp B-3/1 - B-3/36, 1993.
5. H. E. J. Neugebauer, Die Theoretischen Grundlagen des Mehrfarbendruckes, *Z. Wiss. Photogr.* **36**, p 73, 1937
6. R. S. Berns, R. J. Motta and M. E. Gorzynski. CRT Colorimetry. Part I: Theory and Practice, *Color Res. Appl.*, Vol **18**, No 5, pp 299-314, 1993.
7. For example R. S. Berns, "Colorimetric characterization of Sharp JX610 desktop scanner," Tech. rep., Munsell Color Science Laboratory, April 1993.
8. P.-C. Hung, "Colorimetric calibration in electronic imaging devices using a look-up-table method and interpolations," *Journal of Electronic Imaging*, Vol **2**, No 1, pp 53-61, January 1993.
9. H. Motomura, T. Fumoto, O. Yamada, K. Kanamori, and H. Kotera, "CIELAB to CMYK color conversion by prism and slant prism interpolation method," IS&T and SID's Color Imaging Conference: Color Science, Systems and Applications, pp 156-159, November 1994.
10. S. I. Nin, J. M. Kasson, and W. Plouffe, "Printing CIELAB images on a CMYK printer using tri-linear interpolation," *Color Hard Copy and Graphic Arts, SPIE Proc.* Vol **1670**, pp 316-324, 1992.
11. H. Kotera, K. Kanari, and H. Kawakami, "A novel color transformation algorithm and its applications," *Image Processing Algorithms and Techniques*, Vol **1**, pp 272-281, SPIE, 1990.
12. American National Standard IT8.7/2, Graphic technology - Color reflection target for input scanner calibration, 1993
13. A. Albert. *Regression and the Moore-Penrose pseudo-inverse*. Academic Press, 1972.
14. J. Y. Hardeberg, *Transformations and Colour Consistency for the Colour Facsimile*, Diploma Thesis, The Norwegian Inst. of Technology, April 1995.
15. F. Schmitt, H. Maitre, and Y. Wu, *First progress report: tasks 2 and 3.3 - VASARI project*. Technical report, CEE ESPRIT II No 2649, January 1991.
16. F. Schmitt, Y. Wu, J.-P. Crettez, and G. Boulay, "Color Calibration for Color Facsimile," SID International Symposium, Orlando, 1995.

17. L.W. MacDonald, "Gamut mapping in perceptual color space," *IS&T/SID Color Imaging Conference, Transforms and Transportability of Color*, pp 193-196, 1993.
18. K. E. Spaulding, R. N. Ellson, and J. R. Sullivan, "Ultra-Color: A new gamut mapping strategy," *Device Independent Color Imaging II*, vol 2414 of SPIE proc., pp 61-68, 1995.
19. M.C. Stone, W.B. Cowan, and J.C. Beatty, "Color Gamut Mapping and the Printing of Digital Color Images," *ACM Transactions on Graphics*, Vol 7, No 4, pp 249-292, October 1988.
20. A. Bowyer, "Computing Dirichlet tessalation," *Comput. J.*, pp 162-166, 1981.
21. American National Standard IT8.7/3: *Graphic technology - Input data for characterization of 4-color process printing*, 1993.